Myung-Joon Kim, MD
Young Nyun Park, MD
Seok Joo Han, MD
Choon Sik Yoon, MD
Hyung Sik Yoo, MD
Eui Ho Hwang, MD
Ki Sup Chung, MD

Index terms:
Bile ducts, abnormalities, 76.1434
Bile ducts, MR, 76.121411, 76.121412
Bile ducts, radionuclide studies, 76.12172
Bile ducts, US, 76.1298, 76.12983
Gallbladder, 762.1434
Hepatitis, 761.291
Infants, newborn, gastrointestinal tract, 76.1434

Radiology 2000; 215:395–401

Abbreviations:
DISIDA = diisopropyl iminodiacetic acid
SE = spin echo
TE = echo time

[1] From the Departments of Diagnostic Radiology (M.J.K., C.S.Y., H.S.Y.), Pathology (Y.N.P.), Pediatric Surgery (S.J.H., E.H.H.), and Pediatrics (K.S.C.), Severance Hospital, Yonsei University College of Medicine, 134 Shinchon-dong, Seodaemun-ku, Seoul, South Korea 120-752. Received June 29, 1999; revision requested August 12; revision received September 22; accepted September 29. **Address correspondence to** M.J.K. (e-mail: *mjkim@yumc.yonsei.ac.kr*).

Author contributions:
Guarantor of integrity of entire study, M.J.K.; study concepts and design, M.J.K., Y.N.P.; definition of intellectual content, M.J.K., Y.N.P., S.J.H.; literature research, M.J.K., Y.N.P.; clinical studies, M.J.K., Y.N.P., S.J.H.; data acquisition, M.J.K., Y.N.P., S.J.H.; data analysis, M.J.K., Y.N.P., C.S.Y.; statistical analysis, M.J.K.; manuscript preparation, M.J.K., Y.N.P.; manuscript editing, M.J.K., H.S.Y., E.H.H.; manuscript review, M.J.K., Y.N.P., H.S.Y., K.S.C.

Biliary Atresia in Neonates and Infants: Triangular Area of High Signal Intensity in the Porta Hepatis at T2-weighted MR Cholangiography with US and Histopathologic Correlation[1]

PURPOSE: To correlate a triangular area of high signal intensity in the porta hepatis on T2-weighted magnetic resonance (MR) cholangiograms of biliary atresia with ultrasonographic (US) and histopathologic findings in a portal mass observed during a Kasai procedure.

MATERIALS AND METHODS: Twenty-one consecutive neonates and infants (age range, 13–88 days; mean age, 59 days) with cholestasis underwent US and single-shot MR cholangiography. In 12 patients with biliary atresia diagnosed at histopathologic examination, MR cholangiographic findings in the porta hepatis were correlated with US and histopathologic findings in the portal mass.

RESULTS: At US, eight of the 12 patients had round, linear, or tubular hypoechoic portions within a triangular cord; MR cholangiography revealed a triangular area of high signal intensity confined to the porta hepatis. Histopathologic examination of the portal mass revealed a cystic or cleftlike lesion surrounded by loose myxoid mesenchyme and platelike fetal bile ducts. Neither the large cystic lesion without ductal epithelium nor the small cleftlike lesion with scanty epithelium demonstrated bile staining. Similar areas of high signal intensity were not seen on T2-weighted images in the remaining patients (four with biliary atresia and nine with neonatal hepatitis).

CONCLUSION: In biliary atresia, T2-weighted single-shot MR cholangiography can show a triangular area of high signal intensity in the porta hepatis that may represent cystic dilatation of the fetal bile duct.

Ultrasonography (US) and technetium 99m–diisopropyl iminodiacetic acid (DISIDA) imaging are two major diagnostic tools used in the differential diagnosis of neonatal hepatitis and biliary atresia, which are common causes of conjugated hyperbilirubinemia in neonates and young infants (1–6). No single imaging technique can depict the cause in all cases because there is considerable clinical, biochemical, and histopathologic overlap between the two conditions (1–8). Therefore, a multidisciplinary approach to the evaluation of neonatal jaundice is needed to determine the cause of the condition. Endoscopic retrograde cholangiopancreatography is the most useful diagnostic procedure available for direct observation of the extrahepatic bile duct, but it is an invasive procedure that requires infants to undergo general anesthesia, which must be performed by a well-trained endoscopist with the correct instrumentation and technique (9–11).

Magnetic resonance (MR) cholangiography can be applied in pediatric patients with

neonatal cholestasis or choledochal cysts because of the recent development of a half-Fourier acquisition single-shot fast spin-echo (SE) sequence, which is sensitive to static fluid and which can be used to acquire data rapidly (12–16). Although the spatial resolution of MR cholangiography is insufficient for the demonstration of intrahepatic bile ducts in neonates and infants, MR cholangiography can show a normal extrahepatic bile duct, a dilated common bile duct, and the presence of a choledochal cyst (15–20). MR cholangiography can be used to exclude biliary atresia as the cause of neonatal cholestasis when the extrahepatic bile duct is observed (17,20).

In addition to US and ^{99m}Tc DISIDA imaging, we used single-shot MR cholangiography for the differential diagnosis of neonatal cholestasis. We discovered a triangular area of high signal intensity on T2-weighted images that was confined to the porta hepatis in one infant with biliary atresia during the initial period of single-shot MR cholangiography. In fact, this observation motivated us to perform an examination of this area of high signal intensity in the porta hepatis in neonates and infants with neonatal cholestasis. The purpose of our study was to correlate this MR cholangiographic finding with the US and histopathologic features of a portal mass that was observed during a Kasai procedure, that is, an anastomosis of an intestinal loop and the exposed surface of the dissected porta hepatis (hepatoenterostomy).

MATERIALS AND METHODS

Twenty-one consecutive neonates and infants (age range, 13–88 days; mean age, 59 days) who were suspected of having neonatal hepatitis or biliary atresia with persistent cholestatic jaundice at clinical examination were included in this study. All patients were admitted to our hospital and underwent US and ^{99m}Tc DISIDA imaging, which are routine parts of our primary imaging examination. The parents of all patients consented in writing to MR cholangiography for biliary atresia according to the institutional review board–approved protocol (Ethics Subcommittee for Research Involving Human Subjects [no. 99-3], Yonsei University College of Medicine, Seoul, South Korea).

The mean age of the patients at the time of US was 61 days (age range, 13–92 days). The mean time between US and ^{99m}Tc DISIDA imaging was 2 days (range, 0–4 days). The mean age of the patients at

Clinical and Imaging Findings and Final Diagnoses in 21 Patients with Neonatal Cholestasis

Patient No./ Age (d)/ Sex	Level of Serum Bilirubin (μmol/L)		US Findings		Visibility at ^{99m}Tc DISIDA Imaging			Visibility at MR Cholangiography				Final Diagnosis	Bile Duct Size* (μm)
	Total	Direct	Gallbladder Length (cm)	Visible Triangular Cord Sign	Hepatic Extraction of Radiotracer	Gallbladder	Small Bowel	Gallbladder	Extrahepatic Bile Duct	Periportal Thickening	Triangular Area of High Signal Intensity		
1/60/F	273.6	203.5	0.84	Yes	Poor	No	No	Yes	No	Yes	No	Biliary atresia	100
2/57/F	172.7	109.4	2.20	Yes†	Good	No	No	Yes	No	Yes	Yes	Biliary atresia	150
3/80/M	285.6	171.0	1.63	Yes	Poor	No	No	Yes	No	Yes	No	Biliary atresia	150
4/57/M	148.8	116.3	0.50	Yes	Good	No	No	Yes	No	Yes	No	Biliary atresia	40
5/58/F	191.5	136.8	1.50	Yes†	Good	No	No	Yes	No	Yes	Yes	Biliary atresia	120
6/13/F	143.6	78.7	1.66	Yes†	Good	No	No	Yes	No	Yes	Yes	Biliary atresia	140
7/44/F	135.1	95.8	1.09	Yes†	Poor	No	No	Yes	No	Yes	Yes	Biliary atresia	120
8/61/F	159.0	112.9	1.43	Yes†	Good	No	No	Yes	No	Yes	Yes	Biliary atresia	100
9/68/M	184.7	130.0	1.60	Yes	Good	No	No	Yes	No	Yes	No	Biliary atresia	120
10/59/F	153.9	109.4	1.05	Yes†	Good	No	No	Yes	No	Yes	Yes	Biliary atresia	100
11/55/F	213.8	157.3	1.69	Yes†	Poor	No	No	Yes	No	Yes	Yes	Biliary atresia	150
12/40/F	153.9	87.2	2.40	Yes†	NA	NA	NA	Yes	Choledochal cyst	Yes	Yes	Biliary atresia, choledochal cyst	50
13/54/M	121.4	85.5	2.36	No	Poor	No	No	Yes	Yes	No	No	Neonatal hepatitis	. . .
14/68/M	63.3	42.8	2.39	No	Good	Yes	Yes	Yes	Yes	No	No	Neonatal hepatitis	. . .
15/61/M	124.8	54.7	2.16	No	Poor	Yes	Yes	Yes	Yes	No	No	Neonatal hepatitis	. . .
16/69/F	99.2	71.8	1.80	No	Good	Yes	Yes	Yes	Yes	No	No	Neonatal hepatitis	. . .
17/70/F	102.6	73.5	1.41	No	Poor	Yes	Yes	Yes	Yes	No	No	Neonatal hepatitis	. . .
18/88/M	61.6	46.2	2.10	No	Good	Yes	Yes	Yes	Yes	No	No	Neonatal hepatitis	. . .
19/38/M	451.4	309.5	2.90	No	Poor	No	No	Yes	Yes	No	No	Neonatal hepatitis	. . .
20/87/M	136.8	92.3	1.40	No	Poor	No	No	Yes	Yes	No	No	Neonatal hepatitis	. . .
21/54/M	88.9	63.3	1.73	No	Poor	Yes	Yes	Yes	Yes	No	No	Neonatal hepatitis	. . .

Note.—NA = not applicable.
* Diameter of the largest bile duct.
† Hypoechoic or cystic change in a triangular cord.

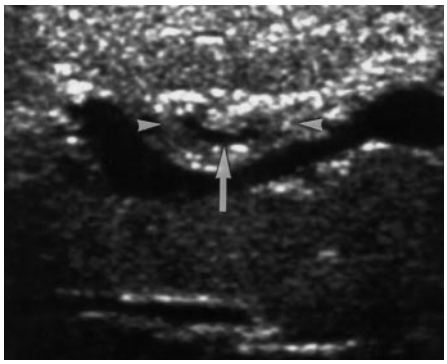

a.

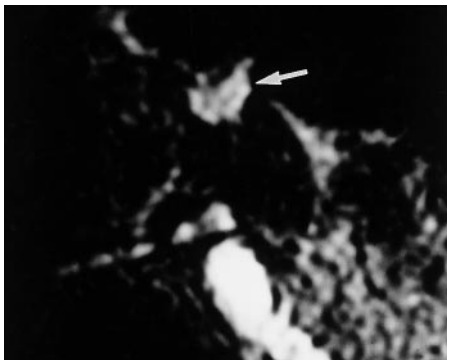

b.

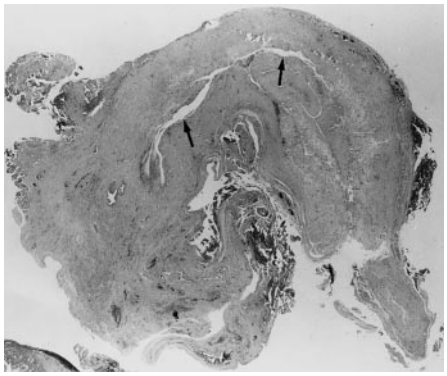

c.

Figure 1. Images obtained in a 13-day-old female neonate with acholic stool. **(a)** Transverse gray-scale US image of the liver shows an echogenic triangular cord (arrowheads) that contains a linear hypoechoic lesion (arrow). **(b)** Oblique coronal thick-slab T2-weighted single-shot fast SE MR cholangiogram (∞/1,257 [effective]) shows a triangular area of high signal intensity (arrow) in the porta hepatis and does not show the extrahepatic bile duct. **(c)** Photomicrograph demonstrates a cleftlike cystic lesion (arrows) within the portal fibrotic mass. The lesion is surrounded by loose and myxoid mesenchyme without lining ductal epithelium. (Hematoxylin-eosin stain; original magnification, ×10.)

the time of MR cholangiography was 64 days (age range, 15–95 days). The mean times between MR cholangiography and US and ^{99m}Tc DISIDA imaging were 2.6 days (range, 0–14 days) and 2.3 days (range, 0–13 days), respectively.

After a minimum 4-hour fast, all patients underwent US with the use of 5–10- and 4–7-MHz transducers (HDI 3000; Advanced Technology Laboratories, Bothell, Wash). US was performed by one pediatric radiologist (M.J.K.). We evaluated the hepatic parenchymal echoes, gallbladder size and shape, and presence or absence of a triangular cord in the porta hepatis. We measured the width and depth of the cord when possible. When abnormal hypoechoic or cystic lesions were noted on the anterior side of the portal venous bifurcation, power Doppler US (pulse repetition frequency, 700–1000 Hz; persistence setting, high; power gain percentage, 75%–80%) was used to exclude vascular structures.

^{99m}Tc DISIDA imaging was performed in all patients with use of a gamma camera (ADAC Vertex EPIC; ADAC Laboratories, Calif). Phenobarbital (Daewon, Seoul, South Korea; 5 mg per kilogram of body weight) was given to each patient for 3–5 days before scintigraphic examination. Patients were not fed for at least 3 hours prior to ^{99m}Tc DISIDA imaging. Approximately 5 mCi (185 MBq) of a ^{99m}Tc DISIDA compound was injected intravenously. Images of the liver, biliary tree, and abdomen were obtained in the anterior projection at 5-minute intervals for the first 60 minutes and at 2, 4, 6, 8, and 24 hours.

Hepatic extraction of the radiotracer, depiction of the gallbladder, and presence of activity in the small bowel were observed on the serial images obtained within 8 hours and on the 24-hour-delay image obtained by an experienced nuclear medicine physician. Poor hepatic extraction was defined as decreased hepatic activity and persistence of cardiac blood-pool activity over 60 minutes. Good hepatic extraction was defined as prompt diffuse hepatic activity with no cardiac blood-pool activity on images obtained at 5–10 minutes.

One hour before the MR imaging examination, patients were sedated with orally administered chloral hydrate (Pocral; Hanlym, Seoul, South Korea; 50 mg/kg). We did not use a negative contrast medium for the suppression of upper gastrointestinal signals. All MR images were obtained with a 1.5-T unit (Signa Horizon; GE Medical Systems, Milwaukee, Wis) with the use of head or knee coils. Before MR cholangiography, we obtained transverse T1-weighted fast multiplanar spoiled gradient-recalled-echo images (180/4.2, repetition time msec/echo time [TE] msec; flip angle, 90°; section thickness, 5 mm; section gap, 1 mm; matrix, 256 × 128; imaging time, 25 seconds) to localize the hepatobiliary system.

MR cholangiography was performed with a T2-weighted single-shot fast SE sequence with thin-section and thick-slab acquisitions. To cover the entire biliary tree, transverse multisection single-shot fast SE images were acquired with the following parameters: ∞/80–100 (effective); echo train length, 128; matrix, 256 × 192; section thickness, 3–4 mm; bandwidth, 31.3 kHz; field of view, 16–20 cm; and mean acquisition time, 36 seconds. When there was an area of abnormal signal intensity anterior to the bifurcation of main portal vein, limited sagittal single-shot fast SE images of the porta hepatis were obtained to further define the relationship with surrounding structures.

Non–breath-hold T2-weighted single-shot MR cholangiography without a respiratory trigger was then performed with a single slab of 20–30-mm thickness (effective TE, 1,100–1,257 msec; echo train length, 128; matrix, 256 × 256; bandwidth, 31.3 kHz; field of view, 14–18 cm; acquisition time, 2 seconds). In all patients, coronal and oblique coronal (−45°, −30°, +30°, +45° to the axis) images were acquired.

Single-shot MR cholangiograms were assessed by two pediatric radiologists, one (M.J.K.) who performed the US examinations and the other (C.S.Y.) who was unaware of the US and ^{99m}Tc DISIDA imaging results. Multisection and thick-slab single-shot MR cholangiograms were analyzed, with an emphasis on the visualization of the extrahepatic bile duct and gallbladder. When the extrahepatic bile duct was indistinct or invisible, specific attention was paid to periportal thickening and the presence or absence of high signal intensity in the porta hepatis on T2-weighted images. The radiologists independently documented the single-shot MR cholangiographic findings and then resolved discrepancies by consensus.

The final diagnosis of biliary atresia and neonatal hepatitis was established at surgery in 12 patients and at liver biopsy in one patient. In these patients, intraoperative cholangiography was performed. One of the 12 patients with biliary atresia also had a choledochal cyst, which was confirmed at intraoperative cholangiography and histopathologic examination.

The remaining eight patients with neonatal hepatitis were diagnosed by means of imaging findings and clinical and laboratory data.

At routine histopathologic examination of the specimens obtained when the Kasai procedure was performed, the portal mass was examined carefully for evidence of cystic changes in the fibrotic mass, and the diameter of bile duct at the porta hepatis was measured. When a cystic space was noted in the fibrotic mass, immunohistochemical staining for cytokeratin was performed to identify remnants of the ductal epithelium.

The Mann-Whitney *U* test was used to evaluate differences in the mean size of the gallbladder in patients with biliary atresia and in patients with neonatal hepatitis. In patients with biliary atresia, the Mann-Whitney *U* test was used to evaluate differences in the mean level of serum bilirubin (total and direct) in patients with and in patients without an area of high signal intensity in the porta hepatis on T2-weighted MR cholangiograms. In patients with biliary atresia, the association between the level of serum bilirubin (total and direct) and the diameter of the largest bile duct at the porta hepatis was analyzed by using the Spearman rank correlation test (SPSS version 7.5; SPSS, Chicago, Ill). A two-tailed *P* value of less than .05 was considered to indicate a statistically significant difference with all tests.

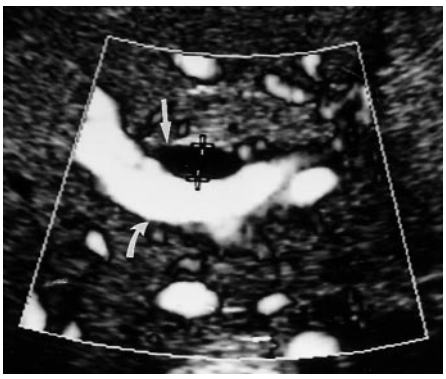

a.

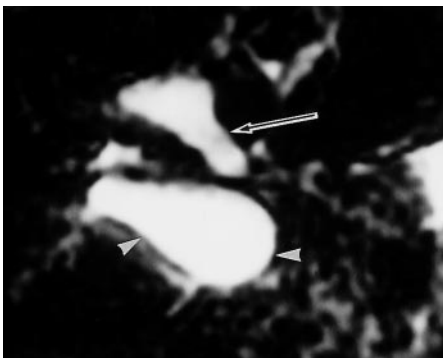

b.

c.

Figure 2. Images obtained in a 57-day-old female infant with cholestatic jaundice and acholic stool. **(a)** Transverse power Doppler US image of the liver shows a tubular cystic lesion (straight arrow), which does not have a flow signal, anterior to the portal vein (curved arrow). Cursors indicate the maximum depth of this cystic lesion. **(b)** Oblique coronal T2-weighted single-shot fast SE MR cholangiogram (∞/1,189 [effective]) demonstrates an inverted triangular area of high signal intensity (arrow) and a normal gallbladder (arrowheads). **(c)** Photomicrograph demonstrates a large cystic lesion (arrows) within the portal fibrotic mass. The lesion is surrounded by a loose myxoid mesenchyme and inflammation. The lining ductal epithelium and bile pigment are absent. (Hematoxylin-eosin stain; original magnification ×10.)

RESULTS

The Table lists the clinical data, including levels of total and direct serum bilirubin, imaging findings, and final diagnoses in the 21 patients with neonatal cholestasis. At US, 12 patients with biliary atresia had a normal parenchymal echo in the liver. A gallbladder with a greatest length of at least 1.5 cm was considered to be normal in size (21,22). According to these US criteria, the gallbladder was small and atretic (0.50–1.43 cm) in five patients and elongated (1.50–2.40 cm) in seven patients. The gallbladders of the patients with biliary atresia were 0.50–2.40-cm long (1.47 cm ± 0.54 [mean ± SD]), whereas those of the patients with neonatal hepatitis were 1.40–2.90-cm long (2.03 cm ± 0.49; Mann-Whitney *U* test, $P < .05$).

In all 12 patients in whom biliary atresia was diagnosed, the triangular cord was depicted at US. The mean width and depth of the triangular cord were 1.89 (range, 1.40–3.20 cm) and 0.47 cm (range, 0.30–0.68 cm), respectively. Among these 12 patients, eight had round, linear, or tubular hypoechoic or cystic lesions within a triangular cord (Figs 1a, 2a, 3a, 4a). At power Doppler US, there was no flow signal within the triangular cords. The remaining four patients had triangular cords without hypoechoic lesions. None of the patients with neonatal hepatitis had the triangular cord (Fig 5a).

In 11 patients with biliary atresia, the gallbladder and small-bowel activity were not visualized at ^{99m}Tc DISIDA imaging at 24 hours. In three of nine patients with neonatal hepatitis, neither the gallbladder nor small-bowel activity were seen at 24 hours. In the remaining six patients with neonatal hepatitis, ^{99m}Tc DISIDA imaging demonstrated the gallbladder and small-bowel activity. Poor hepatic extraction was seen in six patients with neonatal hepatitis and four patients with biliary atresia. Good hepatic extraction was seen in three patients with neonatal hepatitis and seven patients with biliary atresia.

In terms of the diagnostic criteria for biliary atresia, the sensitivity was 100% (11 of 11 patients), the specificity was 67% (six of nine patients), the accuracy was 85% (17 of 20 patients), the positive predictive value was 79% (11 of 14 patients), and the negative predictive value was 100% (six of six patients).

The gallbladder was identified in all patients with biliary atresia at single-shot MR cholangiographic examination. In eight patients who had a hypoechoic or cystic portion within a triangular cord at US, T2-weighted single-shot MR cholangiography demonstrated an area of high signal intensity in the porta hepatis that varied in size. These areas of high signal intensity were just anterior to the portal vein and were easily identified on transverse or sagittal thin-section single-shot fast SE images without superimposition of the areas of signal intensity from the contents of the small bowel, spinal canal, or renal pelvis.

The area of high signal intensity on T2-weighted multisection transverse or sagittal images was ovoid or tubular, but it was always triangular on T2-weighted thick-slab single-shot MR cholangiograms (Figs 1b, 2b, 3b, 4b). In the remaining four patients who had only the triangular cord, T2-weighted single-shot MR cholangiography did not demonstrate a triangular area of high signal intensity. There was no significant difference in the mean level of serum bilirubin between the patients with and the patients without the

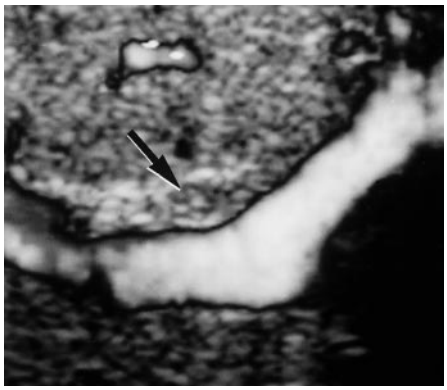

a.

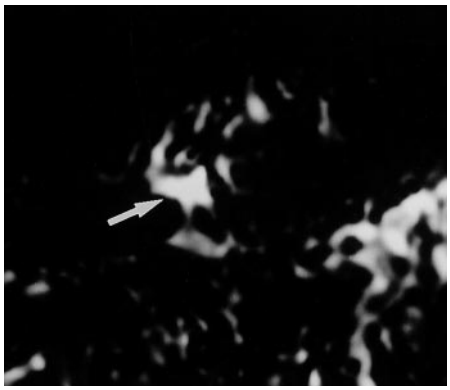

b.

c.

Figure 3. Images obtained in a 59-day-old female infant with persistent jaundice and acholic stool. **(a)** Transverse power Doppler US image of the liver shows a small ovoid hypoechoic lesion (arrow) within a triangular cord that abuts the portal vein. **(b)** Oblique coronal thick-slab T2-weighted single-shot fast SE MR cholangiogram (∞/1,239 [effective]) shows a small triangular area of high signal intensity (arrow) in the porta hepatis. **(c)** Photomicrograph demonstrates a triangular cleft lesion within the portal fibrotic mass, which has some remaining epithelium (arrows) in the bile duct. (Hematoxylin-eosin stain; original magnification ×100.)

area of high signal intensity in the porta hepatis at T2-weighted MR cholangiography (Mann-Whitney *U* test, $P > .05$).

All patients with biliary atresia had periportal thickening on single-shot fast SE images obtained with a short TE. However, periportal thickening was hardly noticeable on single-shot fast SE images obtained with a long TE. On single-shot fast SE images obtained with short and long TEs, the signal intensity of the periportal thickening was less intense than that of the lesions in the porta hepatis. In all patients with biliary atresia except one, in whom biliary atresia was associated with a choledochal cyst (Fig 4b), the extrahepatic bile duct was not depicted at either thin-section or thick-slab imaging. On the other hand, single-shot MR cholangiography in patients with neonatal hepatitis showed a normal extrahepatic bile duct without periportal areas of high signal intensity (Fig 5b).

Intraoperative cholangiography revealed a threadlike common bile duct in two patients with biliary atresia and revealed a choledochal cyst combined with biliary atresia in one. In the remaining nine patients with biliary atresia, intra- and extrahepatic bile ducts were not observed; the contrast medium did not collect in a triangular area around the porta hepatis.

In eight patients who had a triangular area of high signal intensity on T2-weighted single-shot MR cholangiograms, histologic examination of the portal mass revealed cystic or cleftlike lesions within fibrous connective tissue (Figs 1c, 2c, 3c). These lesions were surrounded by a loose myxoid mesenchyme and did not have a lining epithelium; in only one patient did a partial ductal epithelium remain (Fig 3c).

Although multiple serial sections were examined, results of a cytokeratin immunohistochemical staining reaction were negative in most patients. Bile was not found in the lumen or surrounding mesenchyme. Inflammatory reactions in the cysts were scant. Transverse sections of the porta hepatis also showed several structures of the bile duct and bile ductules, which mimicked the structures of the fetal ductal plate. Some of the structures were surrounded by mesenchyme that was similar to that of the larger cystic lesions.

The diameter of the bile duct at the porta hepatis ranged from 40 to 150 μm (111.7 μm ± 36.6). There was no correlation between the level of serum bilirubin (total and direct; $r = 0.386$, $P = .215$) and the diameter of bile duct at the porta hepatis ($r = 0.168$, $P = .601$).

DISCUSSION

The development of a half-Fourier acquisition single-shot fast SE or turbo SE sequence means that the use of MR cholangiography for the investigation of biliary tract diseases in adults has increased (12–16). Authors of published articles (17–20) have described the feasibility of MR cholangiography in children. Guibaud et al (17) stated that biliary atresia could be ruled out if the extrahepatic bile duct is completely identified at MR cholangiography. Chan et al (18) reported that because of the small bile duct and the low rate of bile excretion in neonates and young infants with cholestatic jaundice, MR cholangiography should not be relied on for the demonstration of the bile duct. Both Guibaud et al and Chan et al used a two-dimensional turbo SE sequence with spatial resolutions that ranged from 0.78 to 2.3 mm. Both source images and maximum intensity projections were reviewed. Miyazaki et al (19) used a half-Fourier acquisition single-shot turbo SE sequence with spatial resolutions that ranged from 0.63 to 1.04 mm. They reported that MR cholangiography showed both the first branch of the intrahepatic bile duct and the common bile duct in most children without structural abnormalities. In five patients with biliary atresia, neither the common hepatic duct nor the common bile duct could be seen at MR cholangiography; only a focal rudimentary extrahepatic bile duct was found.

We used a half-Fourier acquisition single-shot fast SE sequence and reviewed both thin-section and thick-slab images. The spatial resolutions we chose for MR cholangiography ranged from 0.55 to 0.70 mm. In our study, the extrahepatic bile duct was identified in all nine patients with neonatal hepatitis. However, in the 12 patients with biliary atresia, MR cholangiography could not depict the extrahepatic bile duct. Areas of high signal intensity from other fluid-containing structures did not affect this finding because thin-section and thick-slab images were obtained at various projection angles in each patient.

In our study, the gallbladder was identifiable at US and MR cholangiography in all patients with biliary atresia. Although we did not measure the size of gallbladder at MR cholangiography, the mean size of the gallbladder in patients with biliary atresia was significantly different from those with neonatal hepatitis, as measured at US.

Periportal thickening related to peripor-

tal fibrosis has been described in patients with biliary atresia and other conditions, which tend to obliterate the bile ducts (8,17,20,23,24). On transverse T2-weighted images, areas of moderately high signal intensity along the portal tract that peripherally extend from the porta hepatis may correlate with periductal edema and inflammatory cell infiltration. In our study, periportal thickening was identified in all patients with biliary atresia. In addition to diffuse periportal thickening, areas of high signal intensity confined to the porta hepatis on T2-weighted images were seen in eight of the 12 patients with biliary atresia. The area of high signal intensity in the porta hepatis was triangular on T2-weighted single-shot MR cholangiograms.

On multisection T2-weighted images obtained with a short TE and on single-slab T2-weighted images obtained with a long TE, the triangular area of high signal intensity in the porta hepatis, which was more intense than that of periportal thickening, appeared to be fluid. US in the eight patients with this finding showed a distinct triangular cord that contained round, linear, or tubular hypoechoic or cystic portions. In the remaining four patients with biliary atresia who had only the triangular cord at US, the area of high signal intensity on T2-weighted images could not be demonstrated on single-shot MR cholangiograms.

In contrast to the patients with biliary atresia, patients with neonatal hepatitis had neither the triangular cord nor the area of high signal intensity in the porta hepatitis on T2-weighted images. This triangular area was not seen in infants or young children who underwent MR imaging for the other hepatobiliary diseases, such as hepatoblastoma, choledochal cyst, or Caroli disease. Therefore, we believe that this signal intensity pattern is specific for biliary atresia.

At ^{99m}Tc DISIDA imaging, drainage of the radiotracer into the small bowel indicates a patent extrahepatic bile duct. However, an image that does not depict draining suggests only that the liver is unable to excrete the radiotracer. Therefore, the specificity of ^{99m}Tc DISIDA imaging in patients with neonatal cholestasis has been reported to be relatively low (75%–100%) (3). Hepatocellular extraction of the radiotracer does not provide an additional marker that allows the discrimination between biliary atresia and neonatal hepatitis (3).

In our study, the specificity of ^{99m}Tc DISIDA imaging was only 67%. Poor hepatic extraction was seen in four patients with biliary atresia, and good hepatic extraction was seen in three patients with neonatal hepatitis. Considering the low specificity of the ^{99m}Tc DISIDA imaging, we believe that the triangular area of high signal intensity in the porta hepatis on T2-weighted MR cholangiograms could provide an additional clue to enable the differentiation of biliary atresia from neonatal hepatitis.

Common histopathologic findings in the tissue samples from the porta hepatis demonstrated that the porta hepatis comprised dense fibrous connective tissue that contained vessels, lymphatics, nerves, and variable degrees of inflammation. Irregular or oval ductlike structures, partially or completely lined with cuboidal or columnar epithelium, were scattered in the portal mass (8,25).

Tan et al (26) compared the developing biliary system in normal human embryos and fetuses with the resected extrahepatic biliary remnants in 205 cases of biliary atresia. There were similarities at immunohistochemical staining for cytokeratin in the abnormal ductules in the porta hepatis with biliary atresia and in the normally developing bile ducts in the first trimester. The authors proposed that an underlying infectious or immunologic injury might cause failure of the remodeling process at the hepatic hilum, with persistence of the poor support of the fetal bile ducts by the mesenchyme. They also found cystic spaces denuded of epithelium in 4% (nine of 205) of the resected specimens (26,27).

In our study, histopathologic examination of the portal mass in eight patients who had the triangular area of high signal intensity on T2-weighted single-shot MR cholangiograms revealed cystic or cleftlike lesions and a loose myxoid mesenchyme in addition to the basic histopathologic features. Bile duct epithelium and bile pigments were absent in all of these cystic lesions except one, which had some remaining epithelium. We did not measure the size of the cystic or cleftlike lesions because of shrinkage and fluid leakage that occurred when the specimens were prepared for histopathologic examination. However, these lesions were much larger than those of the bile ducts at the porta hepatis, so their presence and shape was easily determined at low-power optical microscopy. According to the findings of Tan et al (26,27) and to our histopathologic findings, we postulate that the triangular area of high signal intensity on T2-weighted images of the porta hepatis represents cystic dilatation of the fetal bile duct.

a.

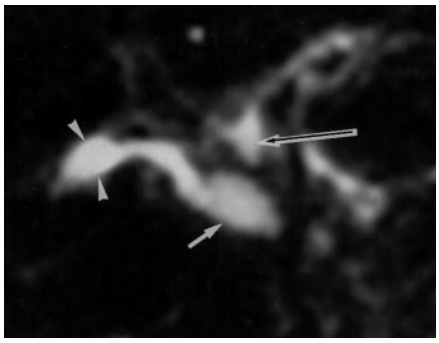

b.

Figure 4. Images obtained in a 40-day-old female infant with jaundice and acholic stool. **(a)** Oblique gray-scale US image of the liver shows a triangular hypoechoic lesion (long straight arrow) within a periportal echogenic mass, a dilated common bile duct (short straight arrow), and the portal vein (curved arrow). Cursors indicate the maximum width (0.79 cm) of the dilated common bile duct. **(b)** Oblique coronal thick-slab MR T2-weighted single-shot fast SE MR cholangiogram (∞/1,100 [effective]) shows a choledochal cyst (short arrow) and the gallbladder (arrowheads). The triangular area of high signal intensity (long arrow) located in the porta hepatis is not continuous with the choledochal cyst or gallbladder. Intraoperative cholangiogram (not shown) demonstrated a choledochal cyst, but the triangular structure at the porta hepatis was not visualized.

There are two shortcomings of this study that should be mentioned. First, one person involved in the evaluation of the MR cholangiographic results was aware of the US results. Second, because a small number of patients had cystic lesions (of unknown clinical importance) within the portal mass that were documented at histopathologic examination, further MR imaging and histopathologic and clinical follow-up examinations are needed.

In conclusion, the triangular area of high signal intensity confined to the porta hepatis on T2-weighted MR cholangiograms in our small population can be used to correctly distinguish biliary atresia from neonatal hepatitis. At histopathologic examination, this signal pattern might represent cystic dilatation of a fetal bile duct.

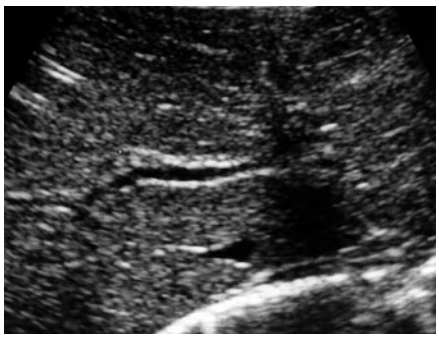

a.

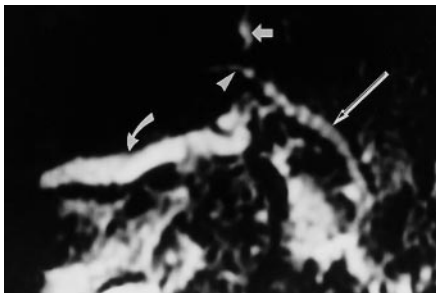

b.

Figure 5. Images obtained in a 69-day-old female infant with neonatal hepatitis. **(a)** Transverse gray-scale US image of the liver shows a normal porta hepatis. The gallbladder is not depicted in this image. **(b)** Oblique coronal thick-slab T2-weighted single-shot fast SE MR cholangiogram (∞/1,257 [effective]) demonstrates a normal gallbladder (curved arrow), common bile duct (long straight arrow), and left intrahepatic duct (short straight arrow) and faintly depicts the right intrahepatic duct (arrowhead).

Acknowledgment: We thank Gye Yeon Lim, MD, for her contribution in one case (patient 12).

References

1. Buonomo C, Taylor GA, Share JC, Kirks DR. Gastrointestinal tract. In: Kirks DR, Griscom NT, eds. Practical pediatric imaging: diagnostic radiology of infants and children. Philadelphia, Pa: Lippincott-Raven, 1998; 954–979.
2. Paltiel HJ. Imaging of neonatal cholestasis. Semin Ultrasound CT MR 1994; 15: 290–305.
3. Gilmore SM, Hershkop M, Reifen R, Gilday D, Roberts EA. Outcome of hepatobiliary scanning in neonatal hepatitis syndrome. J Nucl Med 1997; 38:1279–1282.
4. Lin WY, Lin CC, Changlai SP, Shen YY, Wang SJ. Comparison technique of Tc-99m disofenin cholescintigraphy with ultrasonography in the differentiation of biliary atresia from other forms of neonatal jaundice. Pediatr Surg Int 1997; 12:30–33.
5. Ikeda S, Sera Y, Ohshiro H, Uchino S, Akizuki M, Kondo Y. Gallbladder contraction in biliary atresia: a pitfall of ultrasound diagnosis. Pediatr Radiol 1998; 28: 451–453.
6. Park WH, Choi SO, Lee HJ, Kim SP, Zeon SK, Lee SL. A new diagnostic approach to biliary atresia with emphasis on the ultrasonographic triangular cord sign: comparison of ultrasonography, hepatobiliary scintigraphy, and liver needle biopsy in the evaluation of infantile cholestasis. J Pediatr Surg 1997; 32:1555–1559.
7. Balistreri WF, Grand R, Hoofnangle JH, et al. Biliary atresia: current concepts and research directions. Hepatology 1996; 23: 1682–1692.
8. Chandra RS, Stocker JT. The liver, gallbladder, and biliary tract. In: Stocker JT, Dehner LP, eds. Pediatric pathology. Philadelphia, Pa: Lippincott, 1992; 703–789.
9. Heyman MB, Shapiro HA, Thaler MM. Endoscopic retrograde cholangiography in the diagnosis of biliary malformation in infants. Gastrointest Endosc 1988; 34: 449–453.
10. Derkx HH, Huibregtse K, Taminiau JA. The role of endoscopic retrograde cholangiopancreatography in cholestatic infants. Endoscopy 1994; 26:724–728.
11. Ohnuma N, Takahashi H, Tanabe M, Yoshida H, Iwai J. The role of ERCP in biliary atresia. Gastrointest Endosc 1997; 45:365–370.
12. Barish MA, Soto JA. MR cholangiopancreatography: techniques and clinical applications. AJR Am J Roentgenol 1997; 169: 1295–1303.
13. Jara H, Barish MA, Yucel EK, Melhem ER, Hussain S, Ferrucci JT. MR hydrography: theory and practice of static fluid imaging. AJR Am J Roentgenol 1998; 170:873–882.
14. Reuther G, Kiefer B, Tuchmann A, Pesendorfer FX. Imaging findings of pancreaticobiliary duct diseases with single-shot MR cholangiopancreatography. AJR Am J Roentgenol 1997; 168:453–459.
15. Irie H, Honda H, Jimi M et al. Value of MR cholangiopancreatography in evaluating choledochal cysts. AJR Am J Roentgenol 1998; 171:1381–1385.
16. Matos C, Nicaise N, Deviere J, et al. Choledochal cyst: comparison of findings at MR cholangiopancreatography and endoscopic retrograde cholangiopancreatography in eight patients. Radiology 1998; 209:443–448.
17. Guibaud L, Lachaud A, Touraine R, et al. MR cholangiography in neonates and infants: feasibility and preliminary applications. AJR Am J Roentgenol 1998; 170: 27–31.
18. Chan Y, Yeung C, Lam WWM, Fok T, Metreweli C. Magnetic resonance cholangiography: feasibility and application in pediatric population. Pediatr Radiol 1998; 28:307–311.
19. Miyazaki T, Yamashita Y, Tang Y, Tsushigami T, Takahashi M, Sera Y. Single-shot MR cholangiopancreatography of neonates, infants, and young children. AJR Am J Roentgenol 1998; 170:33–37.
20. Jaw TS, Kuo YT, Liu GC, Chen SH, Wang CK. MR cholangiography in the evaluation of neonatal cholestasis. Radiology 1999; 212:249–256.
21. Kim WS, Kim IO, Yeon KM, Park KW, Seo JK, Kim CJ. Choledochal cyst with or without biliary atresia in neonates and young infants: US differentiation. Radiology 1998; 209:465–469.
22. Kirks DR, Coleman RE, Filston HC, Rosenberg ER, Merten DF. An imaging approach to persistent neonatal jaundice. AJR Am J Roentgenol 1984; 142:461–465.
23. Takahashi A, Hatakeyama S, Suzuki N, et al. MRI findings in the liver in biliary atresia patients after the Kasai operation. Tohoku J Exp Med 1997; 181:193–202.
24. Matsui O, Kadoya M, Takashima T, Kameyama T, Yoshikawa J, Tamura S. Intrahepatic periportal abnormal intensity on MR images: an indication of various hepatobiliary diseases. Radiology 1989; 171: 335–338.
25. Lefkowitch JH. Biliary atresia. Mayo Clin Proc 1998; 73:90–95.
26. Tan CEL, Davenport M, Driver M, Howard ER. Does the morphology of the extrahepatic biliary remnants in biliary atresia influence survival?: a review of 205 cases. J Pediatr Surg 1994; 29:1459–1464.
27. Tan CEL, Driver M, Howard ER, Moscoso GJ. Extrahepatic biliary atresia: a first-trimester event?—clues from light microscopy and immunohistochemistry. J Pediatr Surg 1994; 29:808–814.